Supplementary Information

An anti-freezing, mechanically tough hydrogel via Hydro-Locking for mechanical sensors and flexible supercapacitor at low temperatures

Zeyu Wang[a] ,Xiao Lian[a] ,Jian Lin[a] ， Zhe Huang[a] , Kaixuan Wang[a] , Helin Niu[a,*]

[a] AnHui Province Key Laboratory of Chemistry for Inorganic/Organic Hybrid Functionalized Materials, Key Laboratory of Functional Inorganic Materials of Anhui Province, Department of Chemistry, Anhui University, Hefei 230601, People's Republic of China

*Corresponding Author
E-mail: niuhelin@ahu.edu.cn.

Experimental part

Materials:

Acrylamide (AM, ≥98.0%) was purchased from Tokyo Chemical Industry Co., Ltd. (JP), acrylic acid (AA, RG) from Shanghai Aladdin Biochemical Technology Co. (JP), acrylic acid (AA, RG) was purchased from Shanghai Aladdin Biochemical Technology Co., Ltd, Aluminium Chloride ($AlCl_3$-6H_2O, Bio-Ultra Grade, ≥98.0%) was purchased from Shanghai Adamas Reagent Co. Ltd., 2-hydroxy-4'-(2-hydroxyethoxy)-2-methylpropiophenone (2959 photoinitiator, RG, ≥98.0%) was purchased from Shanghai Adamas Reagent Co., Ltd. and the deionized water was homemade, all the above chemicals were used as received without further purification, unless otherwise stated.

P(AA-co-AM)@Li_3Cit(PCL)Synthesis of Hydrogels:

P(AA-co-AM)@Li_3Cit (PCL) hydrogels were obtained by one-step polymerization using deionized water as solvent. Typically, the P(AA-co-AM)@Li_3Cit (PCL) hydrogels were obtained by adding a certain amount of acrylamide, acrylic acid, and 2959 photoinitiator to a 25 mL round-bottomed flask containing a 1 mol L^{-1} lithium citrate solution, and stirring for 2 h at 40°C.The solution was allowed to dissolve completely by sonication for 30 s. After mixing well, the solution was poured into a mold and irradiated for 70 s under a 40 W UV lamp (365 nm). After complete dissolution and homogeneous mixing, the solution was poured into a mold and irradiated under a 40 W UV lamp (365 nm) for 70 s to obtain P(AA-co-AM)@Li_3Cit (PCL) hydrogels. Due to the absence of cross-linker introduction and the lack of spatially restricted domains in the polymer chains, the synthesized gels took a long time to polymerize, while the mechanical properties were poor and had no resilient properties.

Synthesis of P (AA-co-AM) @ $AlCl_3$-Li_3Cit ($PACL_x$) hydrogel:

PACL is based on PCL hydrogel and aluminum chloride hexahydrate is introduced into the hydrogel. Usually, a certain amount of precursor mixture solution of P(AA-co-AM)@Li_3Cit (PCL) gel was prepared first, and then different mass fractions of aluminum chloride hexahydrate (5 wt%, 15 wt%, 25 wt%, and 35 wt%) were added to the solution with stirring at 40°C in an oil bath for 2 h. After complete dissolution, the precursor solution was poured into molds, and then irradiated by ultraviolet lamp (365 nm) irradiation for 70 s. The P(AA-co-AM)@x$AlCl_3$-Li_3Cit (PACLx) hydrogel was finally obtained. Where x = 5 , 15 , 25 , 35 , represent hydrogels containing 5 wt%, 15 wt%, 25 wt%, and 35 wt% of $AlCl_3$, respectively.

Synthesis of P (AA-co-AM) @ $AlCl_3$ (PAL_{35}) hydrogel:

The PAC is based on a $PACL_{35}$ hydrogel and removes lithium citrate dihydrate from the hydrogel. Generally, this was achieved by adding 35 wt% mass fraction of $AlCl_3$, an amount of acrylamide, acrylic acid, and 2959 photoinitiator to a 25 mL round-bottomed flask containing a 1 mol L^{-1} solution of lithium citrate. The flask was stirred at 40°C for 2 h. The flask was stirred at room temperature(RT) for 3 h or in an oil bath at 40°C for 30 min. After complete dissolution, the precursor solution was poured into a mold and irradiated under UV light (365 nm) for 70 s to obtain the final P(AA-co-AM)@$AlCl_3$ (PAL) hydrogel.

Synthesis of P (AA-co-AM) @ $AlCl_3$-Li_3Cit-D_2O (PACL-D_2O) hydrogel:

The preparation process of PACL-D_2O is similar to that of $PACL_{35}$ hydrogel. Generally, using heavy water as the solvent, this was achieved by adding $AlCl_3$ with a mass fraction of 35%, acrylamide with a mass fraction of 18%, acrylic acid with a mass fraction of 1.8%, and a 2959 photoinitiator to a 25 mL round-bottomed flask containing a 1 mol L^{-1} lithium citrate solution. The mixture was then stirred at 40°C for 2 hours.The flask was stirred at room temperature(RT) for 3 h or in an oil bath at 40°C for 30 min. After complete dissolution, the precursor solution was poured into a mold and irradiated under UV light (365 nm) for 70 s to obtain the final P (AA-co-AM) @ $AlCl_3$-Li_3Cit-D_2O (PACL-D_2O) hydrogel.

Measurement and characterization of $PACL_{35}$ hydrogel:

Fourier transform infrared (FT-IR) spectra were acquired using a Vertex80+Hyperion2000 spectrometer. Low-field nuclear magnetic resonance (LF-NMR) spectra were recorded on an NMI20-15 nuclear magnetic resonance imaging analyzer. Raman spectroscopy measurements were performed with an Xplora Plus in-situ Raman spectrometer. X-ray photoelectron spectroscopy (XPS) data were collected on an ESCALAB 250Xi spectrometer.

Mechanical characterization:

Tensile tests: Hydrogel precursors were solution-cast into Type 1A dumbbell specimens conforming to national standards, and evaluated using a universal testing machine (Instron 5967).

Compression tests: Cylindrical samples (Ø 15.9 mm × height 16 mm) were analyzed under compressive loading on the same Instron 5967 system.

Optical and electrical properties:

Optical transmittance of 2-mm-thick hydrogels was measured with a FluoroMax Plus fluorescence spectrometer. Temperature-dependent conductivity was determined across a broad temperature range using a TH2839 broadband dielectric/impedance spectrometer equipped with a temperature stage. Electrochemical analysis at room temperature was conducted on a CHI760e electrochemical workstation. For Nyquist plot measurements, hydrogel sheets (1 cm × 1 cm × 2 mm) were prepared with copper foil electrodes.

The specific capacitance of the flexible supercapacitor based on $PACL_{35}$ hydrogel is calculated by the following **equation (S1)** :

$$C = \frac{2i_s \int Vdt}{V^2 \mid_{V_i}^{V_f}}$$ **(S1)**

Where *C* is the specific capacitance in F cm^{-2}; i_s is the Current Density in mA cm^{-2} ; *t* is the discharge time in *s*; *S* is the mass of the electrode material in cm^2; and ΔV is the voltage difference in V.

The following equation calculates the energy density (*E*) and power density (*P*) :

$$E = \frac{I \int Vdt}{3.6S}$$ **(S2)**

$$P = \frac{3600E}{\Delta t}$$ **(S3)**

Where *E* is the energy density (Wh cm^{-2}) and *P* is the power density (W cm^{-2}).

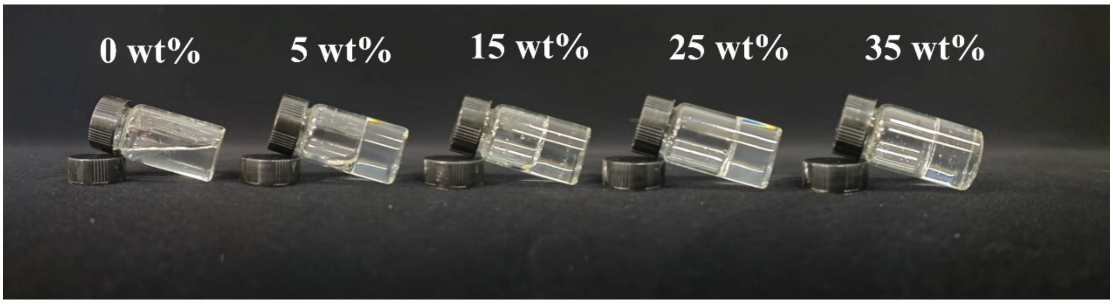

Fig. S1. Comparison of physical images of precursors containing different contents of $AlCl_3$ after initiation under UV lamp for 70 s

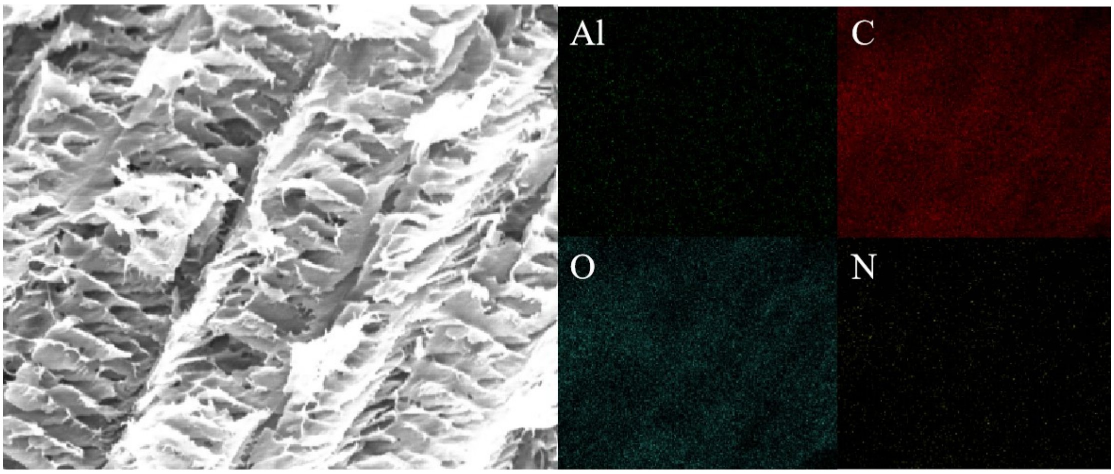

Fig. S2. SEM images confirm the homogeneous distribution of all elements within the hydrogel, directly evidencing the successful synthesis of the material.

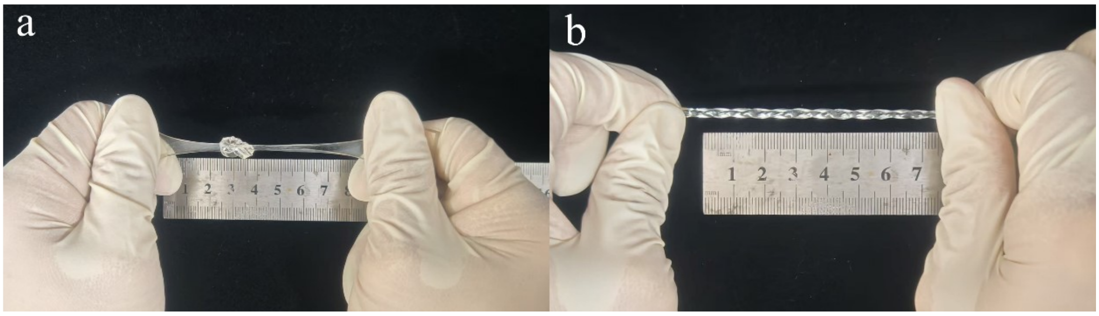

Fig. S3. Schematic representation of a) knotting and b) twisting of $PACL_{35}$ hydrogel

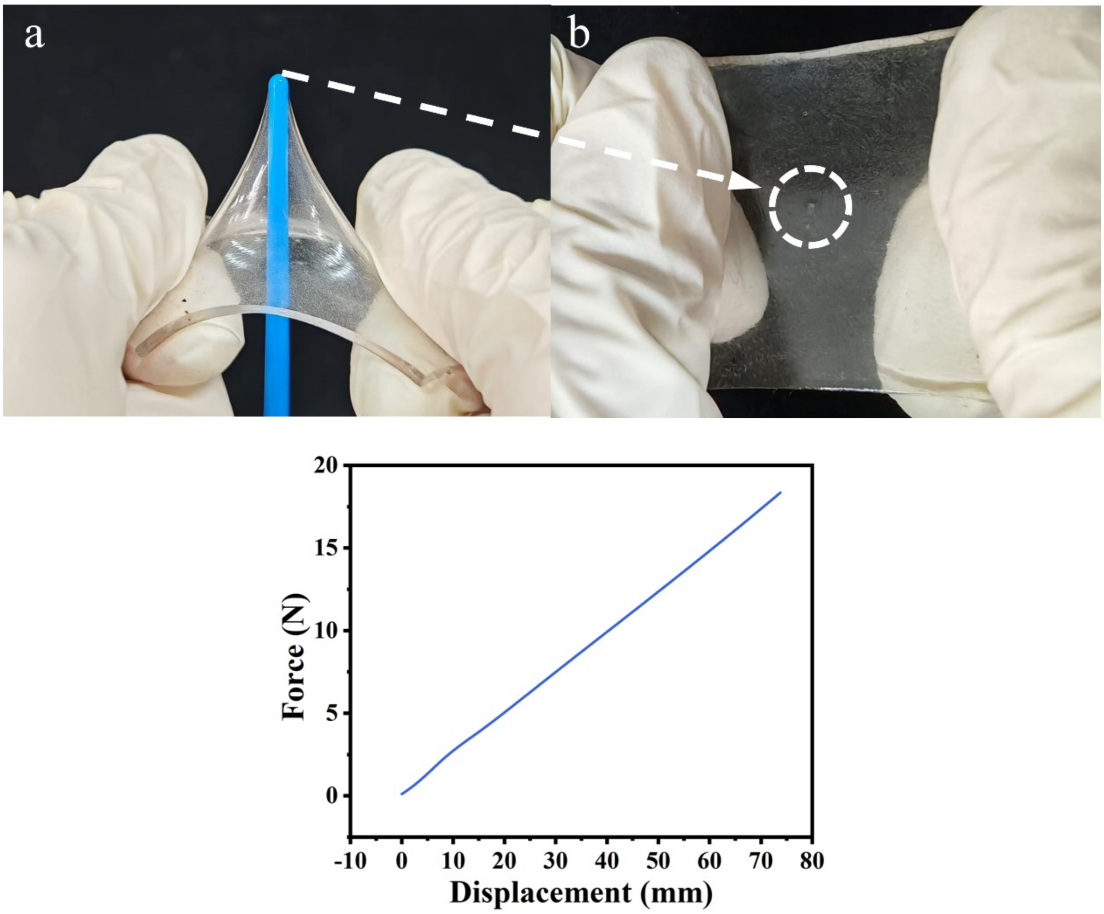

Fig. S4. PACL$_{35}$ hydrogel has excellent puncture resistance

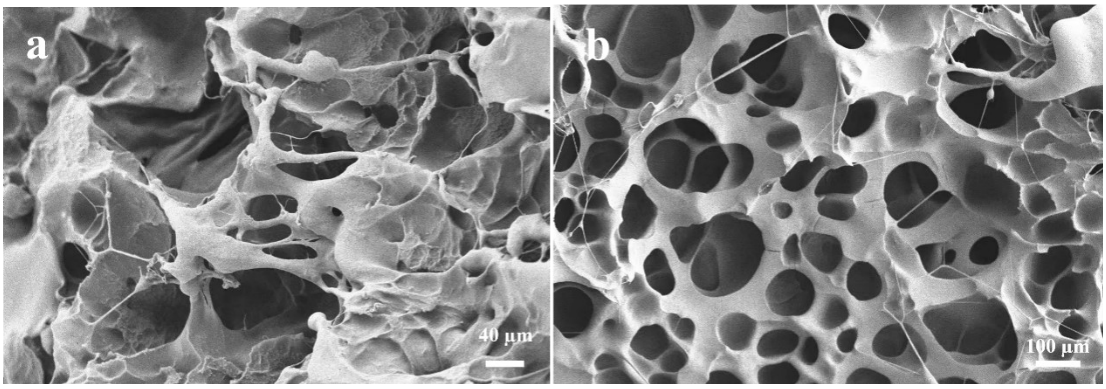

Fig. S5. a) SEM images of PCL hydrogel with only Li_3Cit addition and b) SEM images of PAL_{35} hydrogel with $AlCl_3$ introduced.

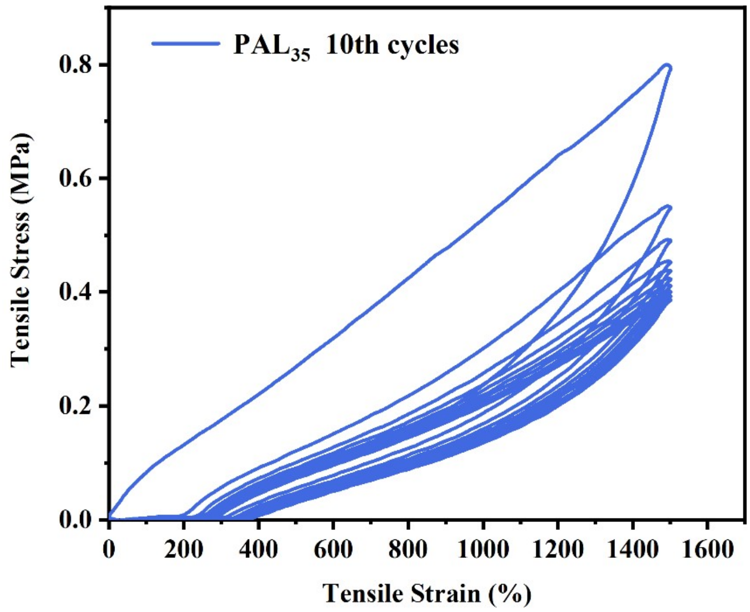

Fig. S6. The cycling performance of the PAL$_{35}$ hydrogel containing only aluminum chloride is obviously weaker than that of the PACL$_{35}$ hydrogel. This is due to the reduction of reversible interactions in the hydrogel caused by the absence of citrate ions.

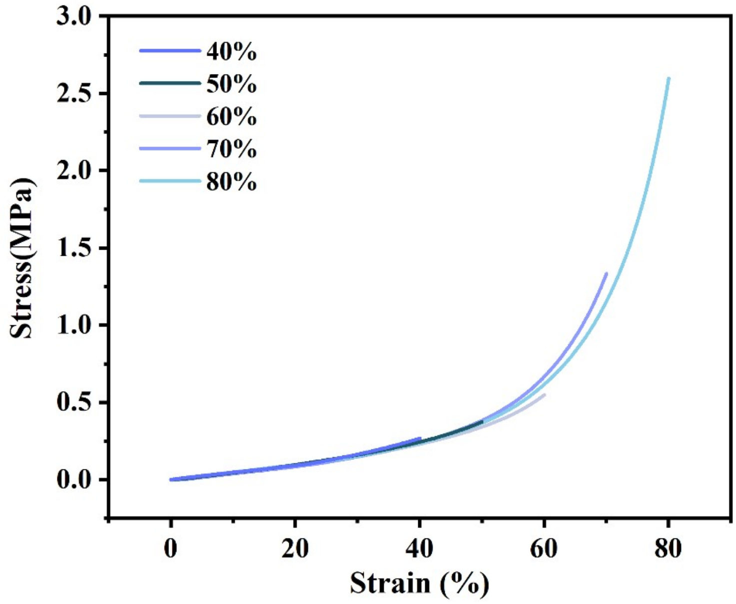

Fig. S7. When $PACL_{35}$ hydrogel was made into cylindrical shapes and subjected to single compressions of different percentages, it was observed that their compression curves basically overlapped, demonstrating the excellent stability of $PACL_{35}$.

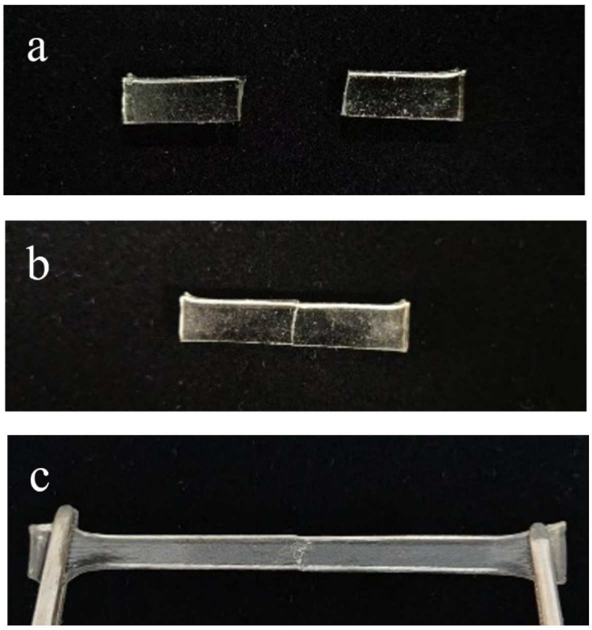

Fig. S8. a) the synthesized hydrogel was cut in half, b) they were tightly contacted and placed together for 8 h, c) the $PACL_{35}$ hydrogel after healing for 8 h was stretched and it was observed that it did not break.

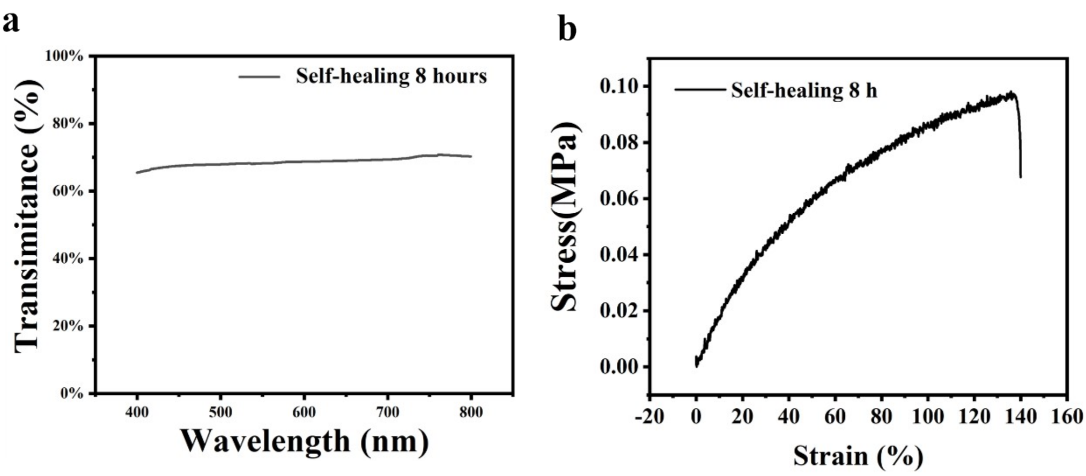

Fig. S9 Changes in light transmittance and mechanical properties of the hydrogel after 8 hours of self-healing

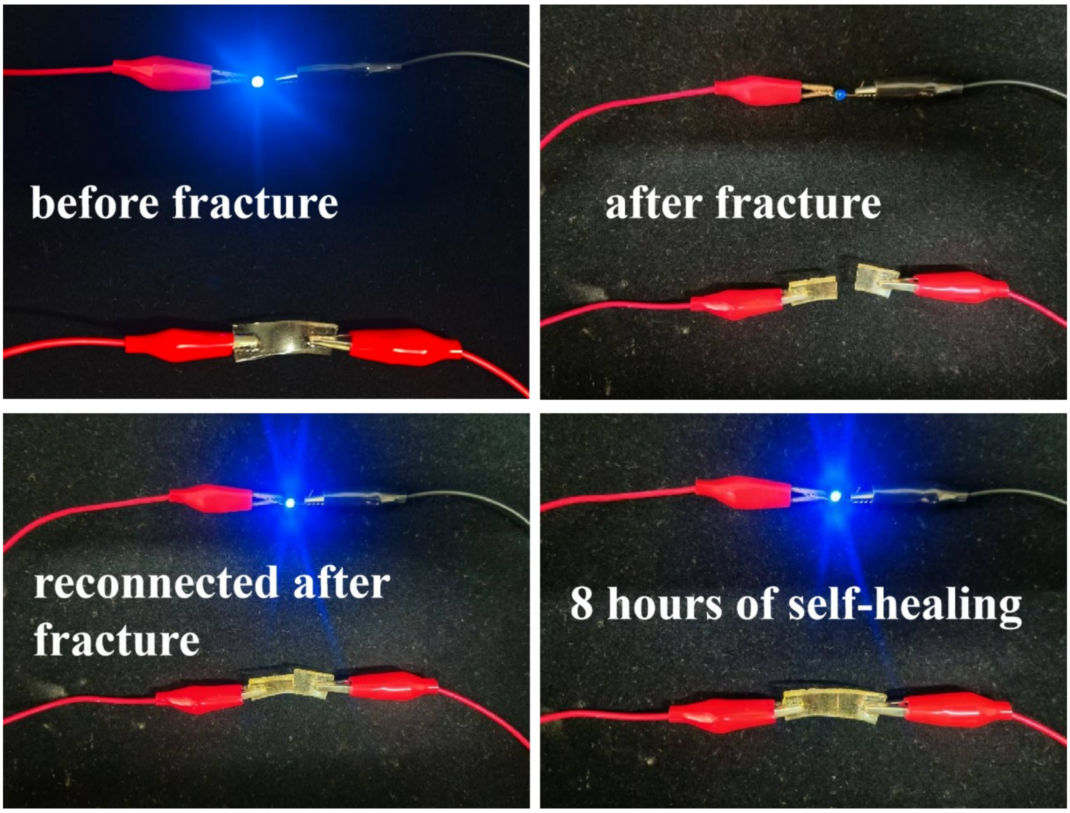

Fig. S10 Conductive property changes of the hydrogel before fracture, after fracture, immediately reconnected after fracture, and after 8 hours of self-healing

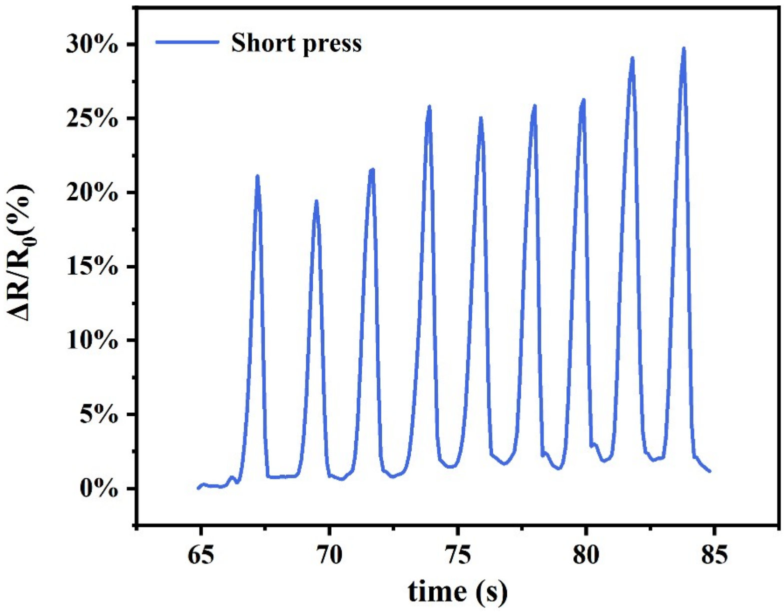

Fig. S11 The $PACL_{35}$ hydrogel exhibits a good and stable electrical signal response to short and brief pressing.

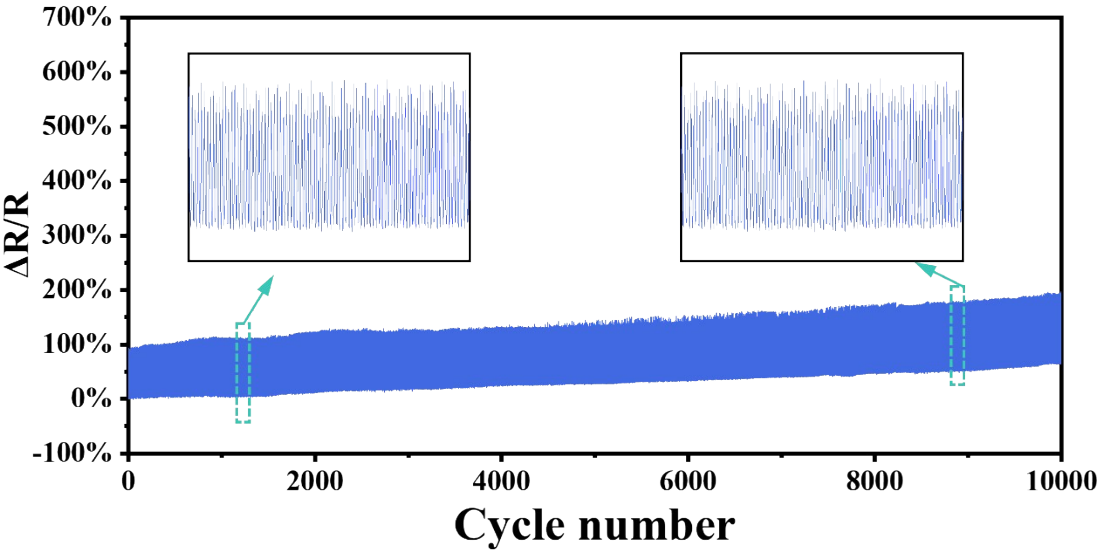

Fig. S12 Electrical signal of $PACL_{35}$ hydrogel under 10,000 cyclic tensile tests

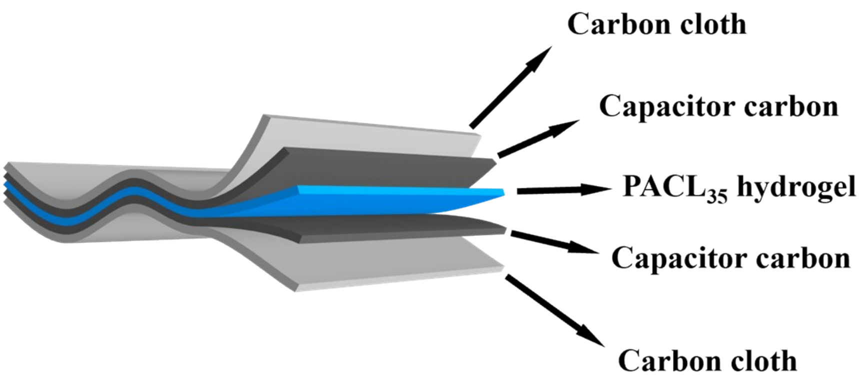

Fig. S13 Structural diagram of supercapacitor

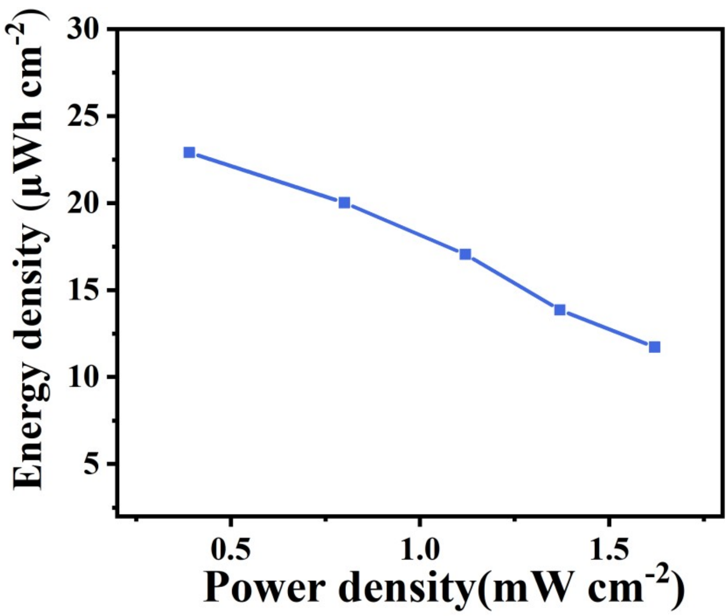

Fig. S14. Ragone diagram of flexible supercapacitors based on $PACL_{35}$ hydrogel

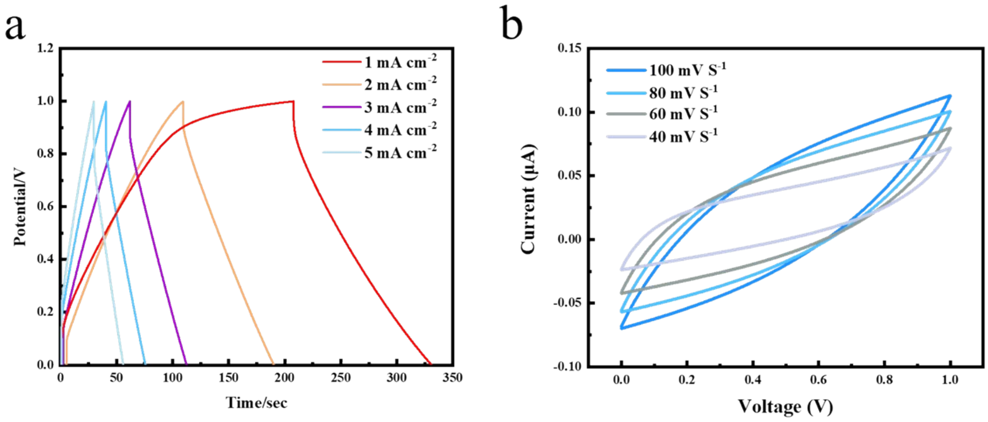

Fig. S14 a) supercapacitor based on a PAL hydrogel containing only AlCl3 has only 50% of the capacitance of a supercapacitor based on a PACL35 hydrogel

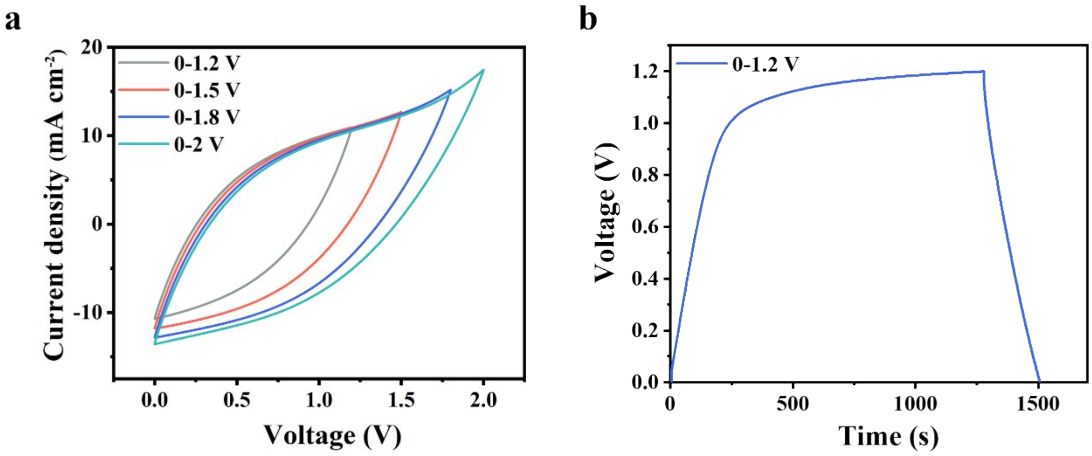

Fig. S15 a) when the voltage window exceeds 1.2 V, the supercapacitor exhibits varying degrees of polarization; b) with the GCD electrochemical window set to 1.2 V, a significant increase in charging time is observed.

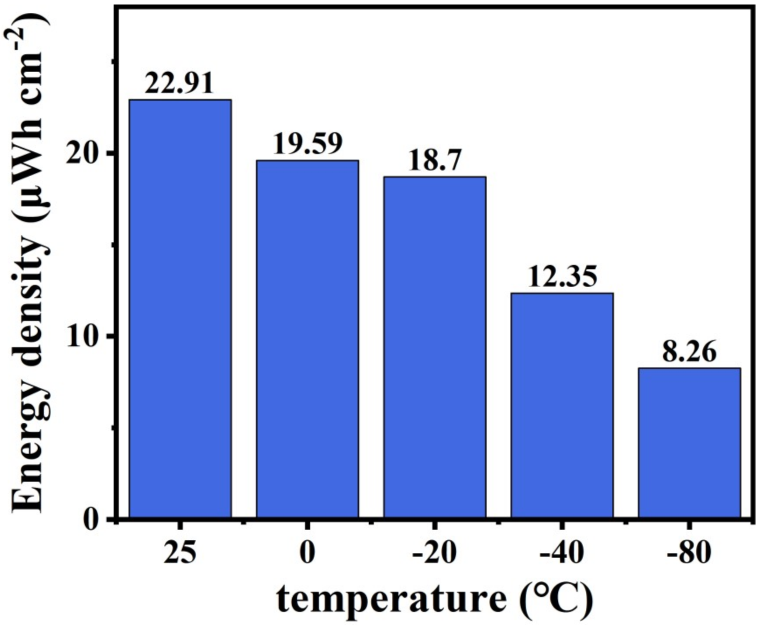

Fig. S16. a) The energy density of flexible supercapacitors at different temperatures shows that they have good low-temperature tolerance.

Table. S1 Comparison of $PACL_{35}$ hydrogel performance with literature reports

Samples	Strain (%)	Stress (kPa)	Anti-freezing (°C)	Conductivity （RT）	Conductivity (-80℃)	Ref
TCPA	863.5%	386.1	-40°C	12.8	—	[1]
DL-$PCaO_2$-PAM	126%	47	-28°C	—	—	[2]
PAAm-CSA	150%	643	-116°C	42.6	0.1 mS cm⁻¹	[3]
PAM/CS–PA	1434%	150.5	Below -60°C	0.87 mS cm⁻¹	—	[4]
HEA-3	979%	46.7	Below -60°C	41.7 mS cm⁻¹	—	[5]
PPM@C-DES	371%	2950	-45.3°C	28.1 mS cm⁻¹	—	[6]
P-KGW	266%	36120	Below -60°C	12.5 mS cm⁻¹	—	[7]
[SL-Fe^{3+}/P]Li	2403%	686	-18°C	25.2 mS cm⁻¹	—	[8]
PAAm+T	4100%	81	-33°C	3.2 mS cm⁻¹	—	[9]
PAM-DVB-Li	5627%	334	-15°C	57 mS cm⁻¹	—	[10]
CS-gel	550%	≈100	Below-150°C	12.7 mS cm⁻¹	0.01 mS cm⁻¹	[11]
$PACL_{35}$	4169%	2150	Below-170°C	67 mS cm⁻¹	0.6 mS cm⁻¹	This work

Table S2 Comparison chart of hydrogel mechanical toughness and cycle numbers

Samples	toughness	number of cycles	Ref
STCHs	3.1 MJ m^{-3}	100s	[12]
PCGEZ-CNTs	4.61 MJ m^{-3}	4000s	[13]
PVA/TOCNF	71.7 MJ m^{-3}	5000s	[14]
NL@PAM	6.61 MJ m^{-3}	100s	[15]
PCSP	3.76 MJ m^{-3}	50s	[16]
C/PVA DN-hydrogel	27.48 MJ m^{-3}	100s	[17]
$PACL_{35}$	29.32 MJ m^{-3}	10000s	This work

[1] Y. Mi, T. Wu, Y. Lu, Y. Wang, Z. Ma, X. Cao, N. Wang, Multifunctional ionic hydrogels with biomimetic stability: Synergistic design and versatile self-powered sensing applications, Chemical Engineering Journal (2025).

[2] C. Xie, S. Jiang, Y. Li, D. Gan, Y. Wang, H. Zhang, J. Weng, Z. Zhang, H. Sun, X. Lu, Self-oxygenating, anti-freezing, antioxidant, and UV-resistant lignin hydrogels for wound healing at high-altitude, Chemical Engineering Journal 517 (2025) 164422. https://doi.org/10.1016/j.cej.2025.164422.

[3] J. Nan, Y. Sun, F. Yang, Y. Zhang, Y. Li, Z. Wang, C. Wang, D. Wang, F. Chu, C. Wang, T. Zhu, J. Jiang, Coupling of Adhesion and Anti-Freezing Properties in Hydrogel Electrolytes for Low-Temperature Aqueous-Based Hybrid Capacitors, Nano-Micro Lett. 16 (2024) 22. https://doi.org/10.1007/s40820-023-01229-9.

[4] Q. Zhang, X. Liu, J. Zhang, L. Duan, G. Gao, A highly conductive hydrogel driven by phytic acid towards a wearable sensor with freezing and dehydration resistance, J. Mater. Chem. A 9

(2021) 22615–22625. https://doi.org/10.1039/D1TA06408H.
[5] J. Liu, Q. Dang, J. Yuwono, S. Zhang, Z. Tai, Z. Guo, Y. Liu, Regulating the Coordination Environment of H2O in Hydrogel Electrolyte for a High-Environment-Adaptable and High-Stability Flexible Zn Devices, Nano-Micro Lett. 17 (2025) 292. https://doi.org/10.1007/s40820-025-01810-4.
[6] W. Wang, Z. Ma, Z. Hu, Y. Long, F. Wu, X. Huang, F.U. Nisa, H. Liang, Y. Dong, J. Wang, M. Tahir, J. Xu, L. He, Synergistic Enhancement of Hole–Bridge Structure and Molecular-Crowding Effect in Multifunctional Eutectic Hydrogel Strain/Pressure Sensor for Personal Rehabilitation Training, Adv Funct Materials (2025) 2502844. https://doi.org/10.1002/adfm.202502844.
[7] Y. Wang, Z. Liu, Y. Liu, J. Yan, H. Wu, H. Zhang, H. Li, J. Wang, H. Xue, L. Wang, Y. Shi, L. Tang, P. Song, J. Gao, Strong, tough and environment-tolerant organohydrogels for flaw-insensitive strain sensing, Mater. Horiz. 11 (2024) 5662–5673. https://doi.org/10.1039/D4MH00740A.
[8] M. Yu, H. Zhang, Q. Yang, N. Li, J. Du, L. Xu, J. Xu, Rapid preparation of tough, anti-freezing, and conductive hydrogel via lignin-Fe3+ self-catalytic system for extreme environment-resistant triboelectric nanogenerator, Chemical Engineering Journal 505 (2025) 159105. https://doi.org/10.1016/j.cej.2024.159105.
[9] Z. Han, P. Wang, Y. Lu, Z. Jia, S. Qu, W. Yang, A versatile hydrogel network–repairing strategy achieved by the covalent-like hydrogen bond interaction, Sci. Adv. 8 (2022) eabl5066. https://doi.org/10.1126/sciadv.abl5066.
[10] R. Wang, P. Chen, X. Zhou, L. Sun, G. Wang, Y. Liu, C. Gao, An Eutectic Gel Based on Polymerizable Deep Eutectic Solvent with Self-Adhesive, Self-adaptive Cold and High Temperature Environments, Adv Materials Technologies 8 (2023) 2201509. https://doi.org/10.1002/admt.202201509.
[11] X. Zhang, D. Li, X. Yang, L. Wang, G. Li, T.-W. Wong, T. Li, W. Yang, Z. Luo, Hydro-locking in hydrogel for extreme temperature tolerance, Science 387 (2025) 967–973. https://doi.org/10.1126/science.adq2711.
[12] M. Hu, Q. Wang, Y. Huang, Z. Lu, Y. Yu, Designing Self-Healing, Printable, and Tough Conductive Hydrogels via the Synergy of Orthogonal Photochemistry and Hofmeister Effect, Macromolecular Rapid Communications n/a (n.d.) e00005. https://doi.org/10.1002/marc.202600005.
[13] Z. Guo, M. Wang, T. Li, S. Xiao, M. Zhou, Y. Li, C. Xia, C. Chen, Q. Fu, Q. Wang, S. Wang, Tough, electron-ion conductive, and anti-freezing cellulose nanofiber reinforced hydrogels inspired by honeycomb as flexible wearable sensors for intelligent human health monitoring, Chemical Engineering Journal 532 (2026) 174479. https://doi.org/10.1016/j.cej.2026.174479.
[14] M. Zhou, L. Wang, Y. Yuan, J. He, H. Zhao, Z. Wang, B. Shang, Z. Peng, H. Wang, L. Huang, Q. Duan, Strong and tough organo-hydrogel enabled by dynamic bonds energy dissipation in chain-aggregated network, Chemical Engineering Journal 532 (2026) 174198. https://doi.org/10.1016/j.cej.2026.174198.
[15] Y. Song, J. Han, B. Wang, S. Li, X. Wang, J. Zhang, N. Li, X. Sheng, H. Shi, C. Shao, R. Sun, Tough and Self-Adhesive Nanolignin Multifunctional Hydrogel-Based Strain Sensor for HumanMachine Interaction, ChemSusChem 19 (2026) e202502341. https://doi.org/10.1002/cssc.202502341.

[16] Y. Su, C. Wang, J. Chen, Y. Zhang, G. Chen, C. Dong, H. Guan, High-strength and tough PPy organohydrogel with electromagnetic shielding in extreme environments and underwater human motion monitoring, Materials Today Chemistry 52 (2026) 103400. https://doi.org/10.1016/j.mtchem.2026.103400.
[17] B. Zhang, X.-X. Chen, X.-R. Ge, X.-P. Wang, X.-H. Yao, W.-G. Zhao, T. Chen, D.-Y. Zhang, Chemically modified bacterial cellulose–mediated fiber salting-out method for preparing tough hydrogels, Carbohydrate Polymers 379 (2026) 124999. https://doi.org/10.1016/j.carbpol.2026.124999.